

## Osmotically driven gelation in double emulsions



Mathieu Delamplé<sup>a,b</sup>, Francielle Da Silva<sup>a</sup>, Fernando Leal-Calderon<sup>a,\*</sup>

<sup>a</sup> Université de Bordeaux, Laboratoire Chimie et Biologie des Membranes et des Nanoobjets, CNRS, Bat. B14, Allée Geoffroy Saint Hilaire, 33600 Pessac, France

<sup>b</sup> AGIR, 37, Avenue Albert Schweitzer, B.P. 100, 33402 Talence Cedex, France

### ARTICLE INFO

#### Article history:

Received 14 September 2013

Accepted 11 November 2013

#### Keywords:

Double emulsions  
Osmotic pressure  
Swelling  
Coalescence  
Gelling

### ABSTRACT

We describe a gelation process based on the osmotically driven water flux between the two aqueous compartments of double emulsions. We first prepare fluid water-in-oil-in-water (W/O/W) double emulsions whose external aqueous phase contains hydrocolloids and/or proteins at moderate concentration. The initial osmotic pressure in the innermost droplets is considerably larger than that in the external phase. An inward water transfer (swelling) is thus likely to occur in order to restore osmotic equilibrium. In the initial state, the globules are large and so the transfer is slow because of the limited exchange surface area. The emulsions are then submitted to a short and intense shear that provokes globule breakup, in order to increase the rate of water diffusion. As a consequence, the initially fluid materials undergo a sudden rheological transition. During that process, the hydrocolloids and/or proteins are concentrated in the continuous phase until a point that a gel is formed. The final rheological properties can be tuned from weak to strong gels depending on the initial composition. The inner droplet fraction strongly increases during the swelling process and droplet–globule coalescence occurs above a critical volume fraction that determines the maximum swelling capacity and thus final state of the system. The proposed approach demonstrates a simple, yet versatile and adaptable solution for making texturized emulsions with reduced fat content and limited amount of hydrocolloids/proteins.

© 2013 Elsevier Ltd. All rights reserved.

### 1. Introduction

Water-in-oil-in-water (W/O/W) emulsions are compartmentalized liquid dispersions in which oil globules, containing small aqueous droplets, are dispersed in an aqueous continuous phase. The presence of inner aqueous reservoirs separated from a continuous phase by an immiscible oil phase enables many potential applications, such as the entrapment of hydrophilic compounds, the partitioning of incompatible substances, the improvement of the performance of active compounds, the sustained release of chemical substances. Multiple W/O/W emulsions have been investigated for usage in pharmaceuticals (Cole & Whateley, 1997; Cournarie et al., 2004; Hino, Yamamoto, Shimabayashi, Tanaka, & Tsujii, 2000; Laugel, Baillet, Youenang Piemi, Marty, & Ferrier, 1998; Tedajo et al., 2005) and cosmetics (Benichou, Aserin, & Garti, 2004; Laugel, Chaminade, Baillet, Seiller, & Ferrier, 1996). Several potential applications have also been envisioned in the food arena for the encapsulation of water-soluble substances like vitamins (Benichou et al., 2004; Fechner, Knoth,

Scherze, & Muschiolik, 2007), or minerals (Bonnet et al., 2009) to implement several strategies such as food fortification or taste masking. More recently, the potentiality of W/O/W emulsions to protect probiotics against the effects of gastric juice and bile acid (Shima, Morita, Yamashita, & Adachi, 2006) was demonstrated. Another promising application is the reduction the caloric intake in dairy products (Lobato-Calleros, Rodriguez, Sandoval-Castilla, Ver-non-Carter, & Alvarez-Ramirez, 2006).

Double emulsions are metastable systems that undergo an inevitable destabilization process provoking structural changes and progressive leakage of the encapsulated actives. The ageing of double emulsions may involve both coalescence and diffusion phenomena. Coalescence consists in the rupture of thin liquid films and may occur at several levels (Florence & Whitehill, 1982; Garti, 1997; Pays, Giermanska-Kahn, Pouligny, Bibette, & Leal-Calderon, 2002): between the inner droplets, between the oil globules, and between the globule and the inner droplets. Hydrophilic species can also migrate from the internal phase to the external one and vice-versa without film rupturing (Benichou et al., 2004; Bonnet, Cansell, Placin, Anton, & Leal-Calderon, 2010; Cheng et al., 2007). The transport is generally driven by concentration gradients of the molecules dissolved in the two aqueous compartments and leads to equilibration of the concentrations.

\* Corresponding author. Laboratoire CBMN (UMR CNRS 5248), Bat. B14, Allée Geoffroy Saint Hilaire, 33600 Pessac, France. Tel.: +33 (0) 5 40 00 68 38.

E-mail address: [fleal@enscbp.fr](mailto:fleal@enscbp.fr) (F. Leal-Calderon).

Water is identically transferred to compensate any transient osmotic pressure mismatch between the two aqueous phases. Water transport rates are affected by numerous parameters. These include the magnitude of the osmotic pressure gradient between the aqueous phases, Laplace pressure, the nature and concentrations of surfactants used for the preparation of the emulsions, the nature and viscosity of the oil phase, etc. (Colinart, Delepine, Trouve, & Renon, 1984; Garti, Magdassi, & Whitehill, 1985; Garti, Romano-Pariente, & Aserin, 1987; Jager-Lezer et al., 1997; Kita, Matsumoto, & Yonezawa, 1978; Matsumoto, Inoue, Kohda, & Ikura, 1980; Matsumoto & Kohda, 1980; Mezzenga, 2007; Mezzenga, Folmer, & Hughes, 2004; Wen & Papadopoulos, 2000). Kita et al. (1978) proposed two possible mechanisms for the permeation of water and water-soluble materials: water molecules (i) pass through the thin liquid film formed by the internal droplets in contact with the globule surface and (ii) diffuse across the oil phase via “reverse micelles”. Colinart et al. (1984) had earlier suggested micellar transport and surfactant hydration as two possible mechanisms for water migration. Garti et al. (1985) and Jager-Lezer et al. (1997) have established that the concentration of oil-soluble surfactant is a major factor for water migration in multiple emulsions and that higher oil-soluble surfactant concentrations yield greater water transport rates.

In a recent article, Leal-Calderon, Homer, Goh, and Lundin (2012) described the fabrication of W/O/W double emulsions with very high internal droplet fraction (more than 90 vol.%) using food-based ingredients. They were able to obtain double emulsions with large globule fractions (up to 45 vol.%) using only 5 vol.% oil (relative to the overall composition). The method was based on two successive emulsification steps in isosmotic conditions, followed by a strong dilution in order to induce osmotic swelling (transport of water from the external phase to the inner droplets). The success of this strategy was based on the fact that migration of water across the oil phase boundary layer is relatively fast compared to the migration of hydrophilic solutes (Matsumoto et al., 1980; Mezzenga et al., 2004). Water migration typically occurs at a time scale of several minutes or hours, whereas migration of hydrophilic solutes such as ions is much slower and can take several days, weeks or even months (Bonnet et al., 2009, 2010; Pays et al., 2002).

Following up on the previous work, here we describe a simple and versatile process to produce food-type gels based on the osmotic swelling taking place in coarse W/O/W emulsions submitted to shear. The proposed approach is relevant within the prospect of creating structured emulsions with novel functional attributes e.g., low fat products with similar sensory qualities as the full fat counterparts. It also aims at exploring novel strategies to trigger textural properties of emulsions with a limited set of additives to meet Clean-Label requirements. The proof of concept was based on double emulsions formulated with sodium caseinate as the hydrophilic emulsifier. This protein was selected because of its specific properties: adsorption at the oil/water interface enabling globule stabilization in the external phase and gelling properties at moderate concentration. Our method exploits the fact that the initial osmotic pressure in the inner droplets is considerably larger than that in the external phase and that excess caseinate is present in the external phase. We initially produce large globules with limited exchange surface area so that the inward osmotically-driven water transfer is slow. The emulsions are then submitted to a short and strong shear in order to induce globule breakup and accelerate swelling. The initially fluid emulsions immediately turn into gels. We propose a description of this phenomenon based on rheological measurements and we examine the key variables allowing a fine-tuning of the gel stiffness. We finally prove the generality of the concept by using hydrocolloids of different types in the external phase.

## 2. Materials and methods

### 2.1. Materials

D-glucose of 99.5% purity and NaCl puriss p.a. were purchased from Sigma (Germany). Both species were used to set the osmotic pressure in the inner aqueous compartments. Sodium azide (NaN<sub>3</sub>, SA) was used as a biocide and was purchased from Merck. The hydrophilic emulsifier, sodium caseinate (SC,  $M_w \approx 20,000 \text{ g mol}^{-1}$ ) was obtained from Lactoprot (Germany). The lipophilic emulsifier was poly-glycerol polyricinoleate, PGPR, (Palsgaard, Denmark). It is made from castor bean oils and is soluble in fats and oils and insoluble in water. As the oil phase, sunflower oil purchased from a local supermarket was used (Lesieur, France, density =  $0.92 \text{ g cm}^{-3}$ , low-shear viscosity ( $1 \text{ s}^{-1}$ ) = 45–50 mPa s). Milli-Q water was used in all experiments.

To probe the generality of the concept, some emulsions were formulated using gum Arabic (from CNI, France), as the hydrophilic emulsifier. Gum Arabic was associated with a thickening/gelling hydrocolloid, Xanthan Keltrol<sup>®</sup> (Kelco U.S. Inc.).

### 2.2. Emulsion fabrication

Emulsification is provoked by the viscous stress applied to the external phase which is transmitted to the droplets. These latter adopt a thread-like shape and are fragmented into smaller droplets (Mabille et al., 2000). In order to produce break-up at relatively low shear rates (laminar regime), a sufficiently large average viscosity is necessary. To fabricate the primary W/O emulsions, this was achieved by adopting a high-dispersed phase content and large PGPR concentration. To disperse the W/O emulsion into the external aqueous phase, the required viscosity level was obtained either by increasing the amount of surface-active species, or by dissolving a thickener in the continuous phase. Mild conditions in terms of applied shear were required during the second emulsification step to preserve the compartmented structure.

For the sake of generality, two series of W/O/W were produced, one containing NaCl and the other D-glucose as the internal solute. Their fabrication involved the 3 following steps carried out at room temperature (20 °C):

**Step 1:** A W/O emulsion was first prepared by drop wise addition of either a D-glucose (40 wt.%) or NaCl (20 wt.%, unless otherwise specified) aqueous phase to an oil phase containing sunflower oil and the emulsifier PGPR at 9 wt.%, under manual stirring. The aqueous phase was incorporated up to 80 wt.% of the total W/O emulsion. The obtained coarse W/O emulsion was then submitted to a strong shear by means of a Couette's cell (concentric cylinders geometry, Ademtech SA, France) (Mabille et al., 2000). The emulsion was loaded in an injection chamber and was syringed in the interspace separating the rotor and the stator. The emulsification was performed with a gap of 100 μm and the applied shear rate was  $1000 \text{ s}^{-1}$ . After this fragmentation step, the emulsions were diluted with sunflower oil and PGPR in order to set the final droplet fraction between 4.8 and 55.6 wt.% as well as the PGPR concentration at 3 wt.%.

**Step 2:** The external aqueous phase was prepared by dissolving SC or a Gum Arabic/Xanthan mixture and 0.02 wt.% SA in water. This solution was gently stirred overnight in order to fully dissolve SC. A coarse double emulsion was fabricated manually by progressive drop-wise incorporation of the previous W/O emulsion into the external aqueous phase, up to an overall concentration varying between 5.25 and 20 wt.%.

**Step 3:** Immediately following its preparation, the W/O/W emulsion was processed in the Couette cell in order to reduce

the globule size and accelerate the swelling process. The applied shear had to be strong enough to provoke globule breakup, while avoiding as much as possible the concomitant shear-induced delivery of the inner droplets reported in many previous studies (Muguet et al., 2001; Stroeve & Varanasi, 1984). The conditions were optimized in terms of applied shear rate to obtain gels with the highest possible rheological moduli within the shortest period of time after the shear was applied. This issue will be further commented at the end of Section 3.4. The following conditions were finally adopted: gap = 100  $\mu\text{m}$ , shear rate = 5000  $\text{s}^{-1}$ , residence time of the emulsion in the cell gap = 5 s.

Table 1 indicates the initial composition of the systems prepared in the course of this study. Once fabricated, the double emulsions were stored at 4 °C for several weeks. This temperature was selected because it corresponds to usual storage conditions for dairy products and also because the kinetic stability was considerably prolonged compared to room temperature.

### 2.3. W/O/W emulsion characterization

The emulsions were observed using phase contrast methods on an Olympus BX51 microscope (Zeiss, Germany) equipped with a video camera. Water droplet size distributions of the primary W/O emulsions were measured by static light scattering, using a Coulter LS 230 apparatus. The measuring cell was filled with sunflower oil containing 1 wt.% PGPR, and a small volume of the sample was introduced under stirring. Measurements were performed at room temperature. The volume weighted average diameter was obtained from Mie theory. The average diameter of oil globules could not be measured using light-scattering because measurements required a strong dilution of the emulsions. Since in our experiments, the final solute concentration in the inner droplets was unknown, it was not possible to match the osmotic pressures in order to avoid water transfer phenomena that would modify the globule size and/or induce coalescence phenomena. The volume-averaged diameter of the globules was thus estimated by direct microscope observations. Images were recorded and the dimensions of about 50 droplets were measured.

**Table 1**

Initial compositions of the W/O/W emulsions formulated within this study (before swelling); SC = sodium caseinate; GA = gum Arabic; X = Xanthan; SA = sodium azide;  $\phi_{i,0}$  = fraction of inner droplets in the globules;  $\phi_{oil}$  = oil fraction;  $\phi_{g,0}$  = globule fraction;  $\phi_{e,0}$  = fraction of the external aqueous phase. All fractions are expressed on a weight percentage basis.

Emulsion n°	Globules				External aqueous phase			
	$\phi_{g,0}^a$	Internal aqueous phase			Oil phase		$\phi_{e,0}^a$	Solute composition <sup>b</sup>
		$\phi_{i,0}^b$	Solute composition		$\phi_{oil}^a$	Composition <sup>b</sup>		
			b	a				
1	5.5%	9.1%	NaCl (20%)	0.1%	5%	Sunflower oil (97%) + PGPR (3%)	94.5%	SC (10%) + SA (0.02%)
2	6%	16.7%		0.2%			94%	
3	7.5%	33.3%		0.5%			92.5%	
4	10%	50%		1.0%			90%	
5	5.25%	4.8%	D-Glucose (40%)	0.1%			94.75%	
6	6.25%	20%		0.5%			93.75%	
7	7.5%	33.3%		1.0%			92.5%	
8	11.25%	55.6%		2.5%			88.75%	
9	10%	50%	NaCl (20%)	1.0%			90%	SC (7.0%) + SA (0.02%)
10								SC (7.5%) + SA (0.02%)
11								SC (8.0%) + SA (0.02%)
12	11.25%	55.6%	D-Glucose (40%)	2.5%			88.75%	SC (7.0%) + SA (0.02%)
13								SC (7.5%) + SA (0.02%)
14								SC (8.0%) + SA (0.02%)
15	20%	50%	NaCl (20%)	2%	10%		80%	SC (10%) + SA (0.02%)
16			NaCl (10%)	1%				GA(10%) + X(2%) + SA (0.02%)

<sup>a</sup> with respect to the total mass of the double emulsion.

<sup>b</sup> with respect to the corresponding phase.

### 2.4. Rheological measurements

When a small shear stress,  $\tau$ , is applied to a solid, the resulting deformation,  $I$ , is proportional to  $\tau$ , with  $\tau = G\Gamma$ , where  $G$  is the elastic shear modulus. For materials which do not store perfectly the energy,  $G$  can be generalized as the sum of two contributions. The in-phase contribution  $G'$  is linked to the stored energy while the  $\pi/2$  out-of-phase contribution  $G''$  is related to the dissipated energy. For complex systems, the relative contributions may be frequency-dependent. Oscillatory rheological experiments were performed with an AR-G2 rheometer from TA-Instruments. The experiments were performed at a frequency of 1 Hz, a strain of 0.5% (linear regime) and at  $T = 4$  °C, using a cone and plate geometry with the following characteristics: cone diameter = 60 mm, cone angle = 2°0'18" and a gap of 56  $\mu\text{m}$ . Since the double emulsions were shear-sensitive, all possible precautions were taken in order to obtain reproducible data. To diminish the "preshear" when loading the samples, the emulsions were loaded into the rheometer very carefully; the sample compression during loading was the minimal possible and was always done at the smallest rate. The lateral parts of the sample were covered by fluid silicon oil to avoid evaporation. All rheological measurements were repeated three times and the deviation between experiments did not exceed 20%.

### 2.5. Density measurements

Unless otherwise specified, the concentrations and droplet/globule fractions will be expressed on a weight percentage basis. The density of all liquids used in the present study (oil, aqueous solutions) were measured at different concentrations in order to convert weight fractions into volume fractions, when necessary. To this end, we used a DMA 4500 density meter from ANTON PAAR (Austria) whose precision is  $\pm 5.10^{-5}$   $\text{g cm}^{-3}$ .

## 3. Results and discussion

### 3.1. Influence of the initial inner droplet fraction at constant oil volume fraction

One of the aims of this study is to fabricate W/O/W double emulsions with the lowest possible oil content. Indeed, low calorie,

kinetically stable food-based double emulsions are highly sought-after and not presently available. In the first set of experiments, all the emulsions were formulated with the same oil content (5 wt.%), the same concentration of SC in the external phase (10 wt.%), but different inner droplet fractions. The initial content of the different systems is indicated in Table 1 (emulsions n°1–8). Despite the very high solute concentration within the inner droplets, the fraction relative to the total emulsion mass never exceeds 1 wt.% for NaCl and 2.5 wt.% for D-Glucose.

The osmotic pressure in the internal aqueous phase,  $\pi_i$ , is elevated owing to the large concentrations and low molar mass of the solutes. Assuming ideal behavior of the solution (van't Hoff approximation), the osmotic pressure can be expressed as:

$$\pi_i = \left( \sum C_i \right) RT \quad (1)$$

where  $R$  is the ideal gas constant,  $T$  is the absolute temperature and  $C_i$  is the molar concentration of the solutes. The summation in Eq. (1) involves all the dissolved species ( $\text{Na}^+$ ,  $\text{Cl}^-$  and D-glucose). The initial osmotic pressure is of the order of  $10^7$  Pa for both types of solutes.

Concerning the external phase, SC dispersions can be considered as a polyelectrolyte solutions and the estimation of their osmotic pressure,  $\pi_e$ , is more complex. The dependence of the osmotic pressure on SC concentration has been measured under variable conditions and ionic strengths (Bouchoux, Cayemite, Jardin, Gésan-Guiziu, & Cabane, 2009; Farrer & Lips, 1999). The following power-law provides a reasonable fit to the data under a large set of conditions and will be adopted hereafter:

$$\pi_e(\text{Pa}) = \alpha[\text{SC}]^\beta, \text{ with } \alpha = 2.51 \times 10^6 \text{ and } \beta = 2.7 \quad (2)$$

where  $[\text{SC}]$  is the weight fraction of protein in the aqueous phase. In the initial conditions,  $[\text{SC}] = 10$  wt.% and we obtain  $\pi_e \approx 5 \times 10^3$  Pa which is 3–4 orders of magnitude lower than the osmotic pressure of the internal phase.

After step 1, daughter W/O emulsions were obtained at variable aqueous droplet fractions upon dilution of mother emulsions at 80 wt.%. The average droplet size deduced from light-scattering measurements was 3.5 and 4.2  $\mu\text{m}$  for NaCl and D-glucose solutions, respectively. These inverted emulsions were in turn emulsified in SC solutions according to the two sequential steps (2 and 3) described in Section 2.2. In Fig. 1, we report macroscopic images of the double emulsion n° 8. The system emulsified manually (step 2) behaved like a viscous fluid that readily flowed when the vial was tipped over (Fig. 1-a). The system was still able to flow after 5 h-storage at room temperature, although we clearly observed a viscosity increase over time reflecting very slow, yet progressive swelling. Right after step 2, the characteristic diameter of the globules was close to 100  $\mu\text{m}$  as can be deduced from the microscope image of Fig. 2-a. At this low magnification, large globules appear as dark spheres because light is scattered multiple times by the inner drops and, as a result, the fraction of transmitted light is quite low. Despite the very large osmotic mismatch between the inner and external aqueous compartments, the swelling process was considerably delayed because of the low surface area of the globules. In such conditions, the globule fraction remained close to its initial value ( $\sim 10$  wt.% in this case) and the viscosity of the emulsion was comparable to that of the external phase (10 wt.% SC aqueous solution), namely 0.1 Pa s at  $10 \text{ s}^{-1}$ . The image of Fig. 1-b was obtained following step 3, about 15 min after the double emulsion was sheared in the Couette cell. The recipient containing approximately 100 mL of emulsion was tilted and the image provides clear evidence that the material did not flow anymore.

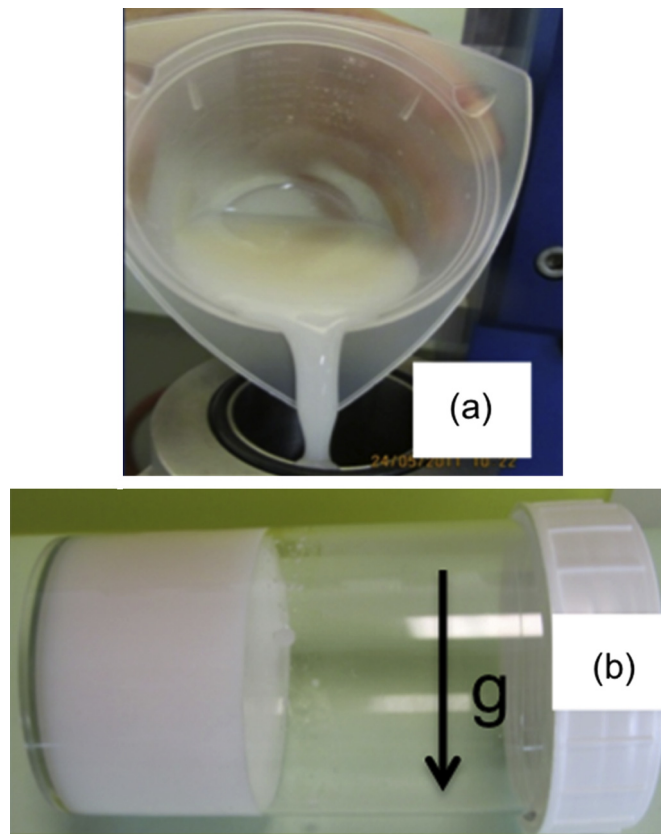
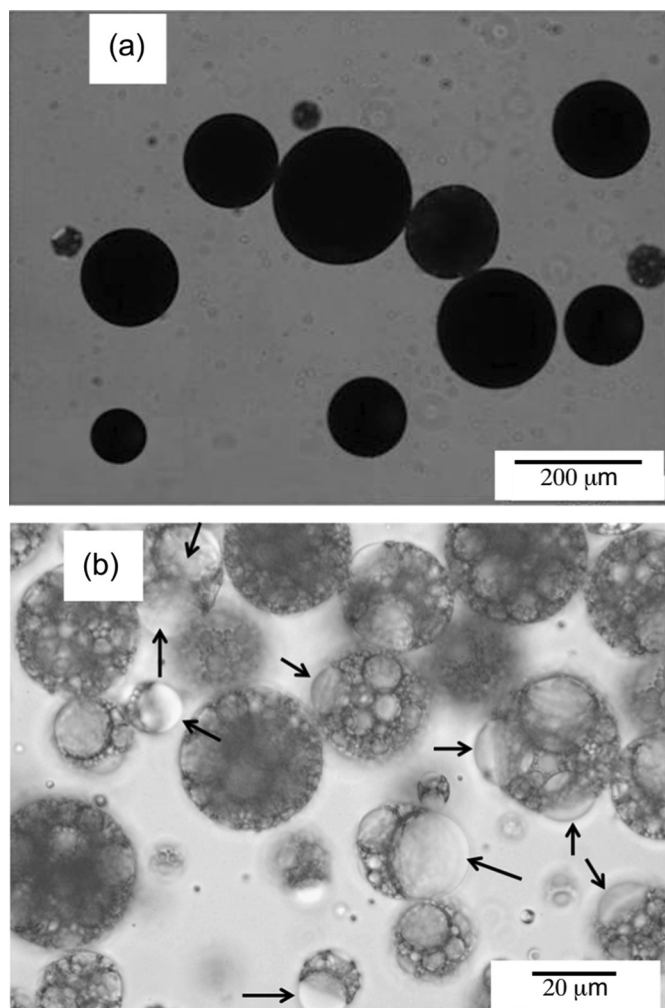


Fig. 1. Macroscopic images of the double emulsion n° 8 (see composition on Table 1) after step 2 (a) and step 3 (b). The arrow indicates the gravity direction.

Instead, it behaved like a strong gel that sustained its own weight without any apparent deformation. Globule fragmentation alone is unlikely to produce such a dramatic rheological change and osmotic swelling must necessarily be taken into consideration.

A small amount of sample was collected and observed under the microscope, revealing the presence of globules whose average diameter was of the order of 20–30  $\mu\text{m}$ . In Fig. 2-b, we can easily distinguish the compartmented structure of the material with tightly packed inner droplets within the globules. Some globules contain internal droplets that are much larger than the average droplet size. This is almost certainly due to coalescence of some of the internal droplets. Interestingly, these large droplets form protrusions, causing the globules to deviate from their native spherical shape because of large compressive forces that deform the globule interface at very high inner droplet fractions. Fig. 2-b thus provides direct evidence that water has been transferred from the external aqueous phase to the internal droplets. The dramatic change in the rheological behavior is probably reflecting the increase of both SC concentration in the external phase and of the globule fraction as a result of the osmotic swelling phenomenon. The shear-induced globule breakup increases the effective surface area for water exchange resulting in a higher inward diffusion rate. The final globule average diameter is thus resulting from two competitive phenomena: the applied shear tends to reduce the globule size, whereas water transfer tends to increase it. It should be underlined that both phenomena are not necessarily occurring at the same time scales. Globule break-up is a shear-induced hydrodynamic (Rayleigh) instability taking place in less than 1 s (Mabille, Leal-Calderon, Bibette, & Schmitt, 2003), whereas osmotic equilibration is expected to occur over a time scale varying from minutes to hours depending on the permeability of oil phase (Mezzenga et al.,



**Fig. 2.** Microscope images of the double emulsion n° 8 (see composition on Table 1) after step 2 (a) and step 3 (b). In Fig. b, the arrows indicate the presence of protrusions on the globules surface.

2004; Wen & Papadopoulos, 2000). The transition from the fluid to the gelled state was observed, irrespective of the initial inner droplet fraction and of the chemical nature of the solute (NaCl or D-glucose). However, we visually observed that the gel firmness increased with the initial inner droplet fraction.

Once processed in the Couette cell, the double emulsions were stored for 15 h at 4 °C. Their mechanical properties were then measured using oscillatory rheology. Fig. 3 shows the dependence of the storage and loss moduli on the initial droplet fraction  $\phi_{i,0}$ . Longer storage periods at 4 °C were experienced (24 and 36 h) and the results were identical within experimental uncertainty. The system corresponding to  $\phi_{i,0} = 0$  can be considered as a control system: it consists of a simple O/W emulsion with 5 wt.% oil dispersed in the aqueous phase containing 10 wt.% SC and 0.02 wt.% SA. The rheological moduli of the double emulsions are 2–3 orders of magnitude larger than those of the control emulsion and for most of the systems under study  $G'$  becomes larger than  $G''$  reflecting the predominantly elastic nature of the materials. The curves obtained for D-glucose (Fig. 3-a) and NaCl (Fig. 3-b) exhibit similar trends: the larger the initial droplet fraction, the larger the rheological moduli become although the variations seem moderate because of the log-scale adopted for the ordinate.

To provide further evidence that the gelled state is resulting from the compartmented structure and the inward water flux, we

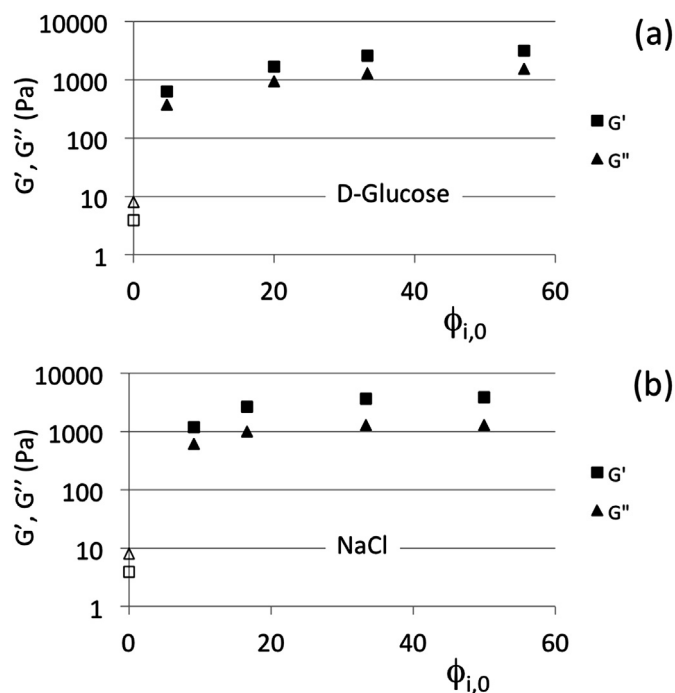


**Fig. 3.** Variation of the rheological moduli  $G'$  et  $G''$  as a function of the initial droplet volume fraction; inner solute = D-glucose (emulsions n° 5–8) (a); NaCl (emulsions n° 1–4) (b). The initial compositions of the emulsions are provided in Table 1. Open symbols correspond to a solution with 10 wt.% SC and 5 wt.% oil dispersed in it.

fabricated an emulsion in one step with exactly the same components and the same contents as in emulsion n° 8. An aqueous phase containing all the hydrophilic species (D-Glucose + SC + SA) and an oil phase with 3 wt.% PGPR were first prepared. Both phases were mixed manually and sheared at  $5000 \text{ s}^{-1}$  in the Couette cell. The resulting material was a fluid O/W emulsion with a viscosity comparable to that of the 10 wt.% CS solution.

### 3.2. Influence of initial sodium caseinate concentration in the external phase at constant globule and inner droplet fractions

In this second series of experiments, we maintained the same initial inner droplet fraction (50 wt.%) and the same globule fraction (10 wt.%), and we varied the concentration of SC in the external phase from 7 to 10 wt. %. It was not possible to lower the concentration further than 7 wt.% because the viscosity was insufficient to maintain sample homogeneity during step 3. Indeed, for  $[\text{SC}]_0 < 7 \text{ wt.}\%$ , the large globules ( $>100 \mu\text{m}$  on average) resulting from step 2 tended to sediment after a few minutes, which was the delay required to syringe the whole amount of emulsion through the gap of the Couette cell. We preferred discarding emulsions that were not spatially homogeneous during step 3.

Fig. 4 shows the variations of  $G'$  and  $G''$  in the final state at 4 °C. Both moduli vary over almost 2 decades within the relatively narrow range in SC concentration, reflecting the strong sensitivity of the gel properties with respect to this compositional variable. The gel is mostly dissipative ( $G'' > G'$ ) for  $[\text{SC}]_0 = 7 \text{ wt.}\%$ . In this limit, the obtained material is able to flow under the effect of its own weight (Fig. 5-a). Conversely, the materials become elastically-dominant ( $G' > G''$ ) for  $[\text{SC}]_0 > 7.5 \text{ wt.}\%$ . For  $[\text{SC}]_0 = 10 \text{ wt.}\%$ , the yield stress becomes high enough to hinder the gravity induced flow in vials containing  $\sim 100 \text{ mL}$  (Fig. 5-b). Again, the same qualitative effect is obtained for the two types of inner solutes (D-glucose (Fig. 4-a) and NaCl (Fig. 4-b).

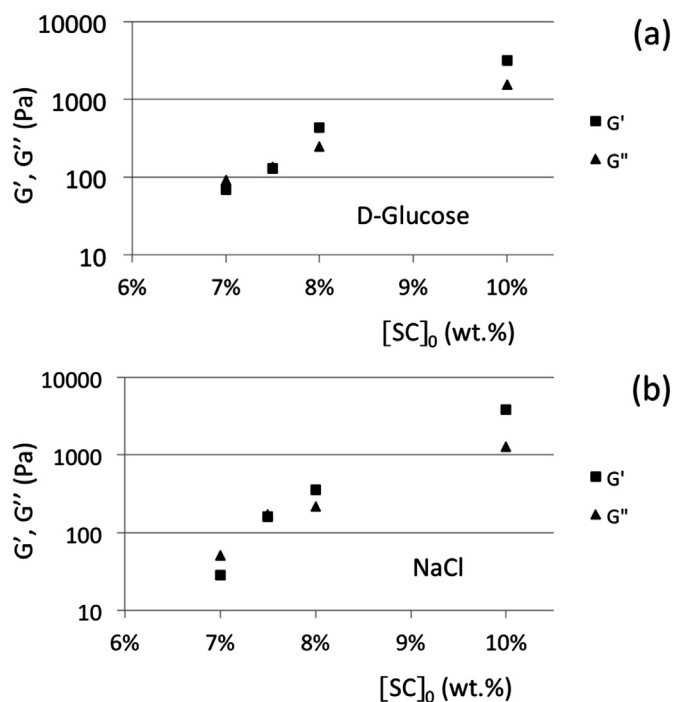


Fig. 4. Variation of the rheological moduli  $G'$  et  $G''$  as a function of the initial SC concentration in the external phase; inner solute = D-glucose (emulsions n° 8, 12, 13, 14) (a); NaCl (emulsions n° 4, 9, 10, 11) (b). The initial compositions of the emulsions are provided in Table 1.

In principle  $G'$  and  $G''$  are expected to depend on the final concentration of SC in the external phase, on the globule fraction and on the interactions between the globules. The coupling between these variables and their dependence on  $\phi_{i,0}$  and  $[SC]_0$  is non trivial and makes any theoretical prediction cumbersome. Hereafter, we propose an analysis based on simplifying – yet realistic – assumptions aiming at better understanding the phenomena that control the final material properties.

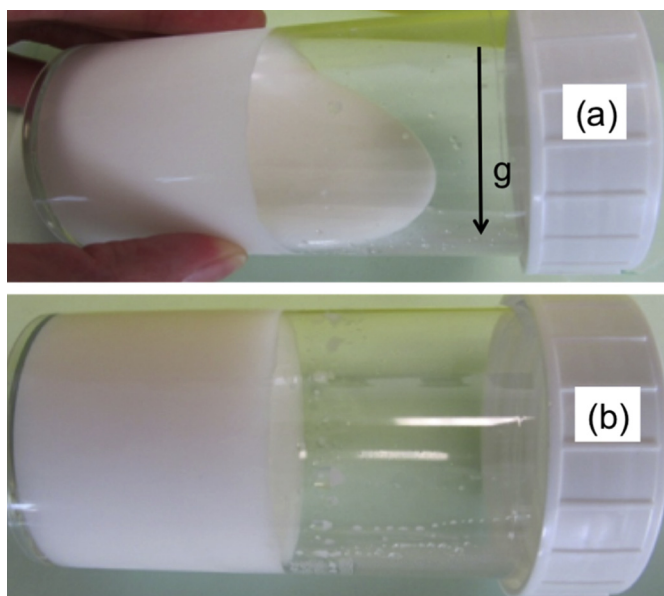


Fig. 5. Macroscopic images of the double emulsions n° 9 (a) and n° 4 (b). The arrow indicates the gravity direction. The initial compositions are provided in Table 1.

### 3.3. Analysis based on osmotic equilibration

We first hypothesize that the final state is determined solely by water transfer phenomena. Within this approach, it is assumed that no coalescence of the inner droplets on the globule surface occurs following the significant volume expansion and that the solutes do not migrate across the oil phase within the time-scale of the experiments.

The driving force for the swelling process is the osmotic pressure difference,  $\Delta\pi = \pi_i - \pi_e$ , caused by the different compositions of the aqueous solutions. The osmotic swelling is counter balanced by surface tension. As the internal droplets inflate, their interfacial area and thus their surface energy increases. Provided that a valid expression for  $\Delta\pi$  is found, it is possible to calculate the average diameter of the internal droplet at equilibrium,  $d_d$ , by solving equation (3) (Mezzenga et al., 2004):

$$\Delta\pi = \frac{4\sigma}{d_d} \quad (3)$$

where  $\sigma$  is the interfacial tension between oil and the aqueous phase and the osmotic pressures are given by equations (1) and (2). The total volume  $V_w$  of the aqueous phase remains constant, which provides a useful closure relation:

$$V_w = V_i + V_e \quad (4)$$

$V_i$  and  $V_e$  being the volumes of the internal and of the external aqueous phases respectively. The set of equations (1)–(4) can be solved numerically in order to determine the composition of the system at osmotic equilibrium. Considering the conditions adopted in the present study ( $\sigma \approx 2$  mN/m (Marze, 2009),  $d_d \geq 5$   $\mu$ m), both  $\pi_i$  and  $\pi_e$  are at least two orders of magnitude larger than Laplace pressure ( $4\sigma/d_d$ ) at equilibrium. Thus, the equilibrium condition can be simply expressed as  $\pi_i \approx \pi_e$ .

In Fig. 6, we report the theoretical variation of the concentration of SC in the external phase after osmotic equilibration, under the different initial configurations that were probed in the previous sections: variable inner droplet fraction at constant oil volume fraction (Fig. 6-a) and variable SC concentration in the external phase at constant globule and inner droplet fraction (Fig. 6-b). The inserts show the variation of the inner droplet fraction after osmotic equilibration, defined as:

$$\phi_i = \frac{V_i}{V_i + V_{oil}} \quad (5)$$

where  $V_{oil}$  is the volume of the oil phase. Because of the very low osmotic pressure of the external phase compared to the internal one in the initial conditions, the extent of swelling predicted by this model is remarkably high as revealed by the very large equilibrium values of  $[SC]$  and  $\phi_i$  (solid lines).

Unfortunately, it was not possible to directly measure  $[SC]$  in our double emulsions because of their very large viscosity. Collecting the continuous phase required a long and high-speed centrifugation step, which inexorably led to globule compression and partial destruction of the double structure with significant release of the inner droplets. In order to assess the pertinence of this approach, we measured the variation of  $G'$  and  $G''$  in aqueous solutions containing a well-defined amount of SC, and 0.02 wt.% SA (Fig. 7). Samples with high SC concentrations were difficult to homogenize and the upper explored limit was 20 wt.%. Assuming that the rheological properties of the double emulsions are determined by the continuous phase, the plot of Fig. 7 can be considered as a calibration curve. We are aware that this is an oversimplifying approach as the globules also contribute to the rheological

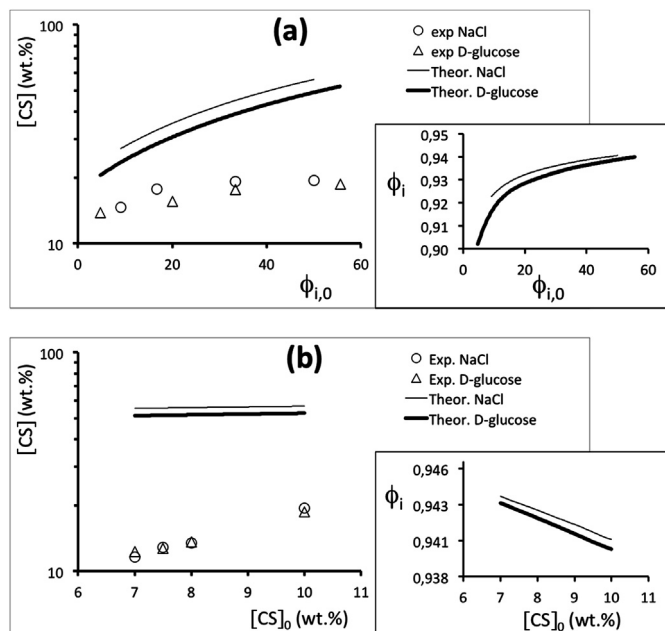


**Fig. 6.** Variation of the SC concentration in the external aqueous phase after osmotic equilibration under variable initial conditions; (a) constant oil content and variable inner droplet fraction; (b) constant globule and inner droplet fraction and variable sodium caseinate concentration. Solid lines are theoretical predictions. The points correspond to the experimental upper limit deduced from the calibration curve of Fig. 7 (see text for details). Insert: internal droplet fraction (theoretical).

properties, in addition to the continuous phase. We dispersed sunflower oil in the SC solutions and we systematically observed an increase of the rheological moduli compared to the system devoid of droplets. For instance for  $[SC] = 15$  wt.%, we observed a 10% increment in  $G'$  of the emulsion containing 40 wt.% oil droplets of  $30 \mu\text{m}$  compared to the simple SC solution. Thus, this calibration method necessarily leads to an upper (overestimated) value for  $[SC]$  and  $\phi_i$  after equilibration. Despite the intrinsic overestimation, the corresponding points reported in Fig. 6 (calibration based on  $G'$ ) are well below theoretical predictions (solid lines). This gives a hint that a model merely based on osmotic equilibration is not appropriately predicting the final state of the system.

#### 3.4. Analysis based on osmotic swelling followed by coalescence

It has been demonstrated (Matsumoto & Kohda, 1980; Raynal et al., 1994) that strong osmotic pressure gradients cause the

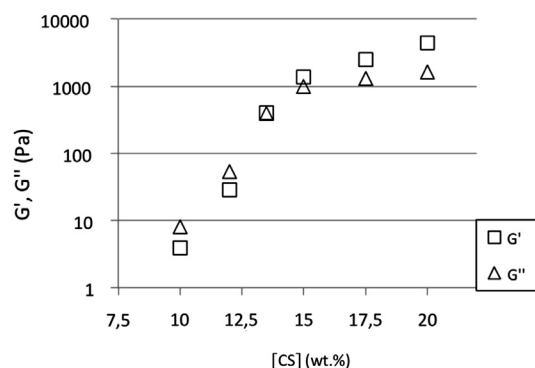


**Fig. 7.** Variation of  $G'$  and  $G''$  for aqueous solutions containing 0.02 wt.% SA and different SC concentrations.

internal aqueous droplets to swell until a point they are strongly compressed and coalescence occurs on the globule surface. This phenomenon, hereafter referred to as “droplet–globule coalescence”, leads to the full release of the internal droplet content into the external aqueous phase. Identically, Leal-Calderon et al. (2012) provided evidence that droplet–globule coalescence occurs in double emulsions submitted to a strong osmotic shock and that such phenomenon is strongly influencing the final state of the system. On the one hand, they were able to collect and analyze the continuous phase and they observed that the solute concentration was always lower than predicted. On the other hand, they carried out experiments in which the initial osmotic pressure mismatch was extremely large, like in the present study. The swollen globules were prone to creaming owing to the relatively low viscosity of the external phase. After a few hours of settling, they formed a layer sitting at the top of the recipients and coexisting with a transparent aqueous subnatant phase. The thickness of the cream layer was taken as an indicator of the extent of swelling. The relative cream thickness (height of the cream normalized by the total sample height) was always lower than the theoretical globule fraction based on the above-described osmotic equilibration model, despite the globules only occupy a fraction of the creamed volume (50–60%). The authors concluded that the amount of internal water released through coalescence was significant, resulting in a relatively low final globule fraction. The amount of inner aqueous phase released through coalescence was estimated from very simple geometrical considerations and it turned out that such amount increased with the initial osmotic pressure mismatch.

The discrepancy between the theoretical predictions and the data deduced from the calibration curve in Fig. 6 is most likely due to coalescence phenomena taking place between the inner droplets and the globule surface. Inner droplets are tightly packed upon swelling and experience large compressive forces that may produce both droplet–droplet and droplet–globule coalescence. For the sake of simplicity, we assume that droplet–globule coalescence occurs above some critical inner droplet fraction  $\phi^*$  (Leal-Calderon et al., 2012). We are thus considering a limit where the initial osmotic mismatch is so large that the final state is determined not by osmotic conditions but by thin film stability criteria. The inward flux increments the inner droplet fraction without droplet–globule coalescence up to the critical fraction  $\phi^*$ . Then, swelling and coalescence compensate each other thus maintaining the inner droplet fraction equal to  $\phi^*$  before complete osmotic equilibration is achieved. Within this simple approach, the amount of water transferred,  $\Delta V$ , from the outer to the inner aqueous phase only depends on  $\phi^*$ :

$$\Delta V = \frac{\phi^* (V_{i,0} + V_{oil}) - V_{i,0}}{1 - \phi^*} \quad (6)$$

where the subscript “0” refers to the initial state. The final concentration of SC in the continuous phase is then straightforwardly derived. We tried to fit the experimental data of Fig. 6 using  $\phi^*$  as the unique free parameter. The obtained values for  $\phi^*$  are reported in Fig. 8 (versus  $\phi_{i,0}$  (a) or  $[SC]_0$  (b)). Considering the previous remarks about the overestimation of  $[SC]$ , the ordinate of the graphs represent an upper limit for  $\phi^*$ . However, it should be underlined that the obtained values are very similar to those deduced from direct measurements by Leal-Calderon et al. (2012) for similar W/O globules (same oil type and same PGPR concentration).

In Fig. 8-a,  $\phi^*$  exhibits a slight but regular increase with  $\phi_{i,0}$  probably reflecting the variation of the average inner droplet size. As explained in the materials and methods section, for a given solute (NaCl or D-glucose), all the W/O emulsions derive from the

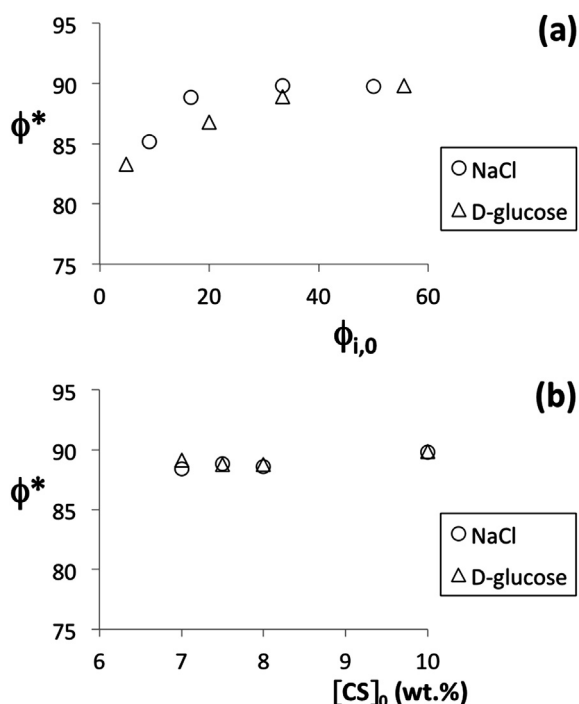


**Fig. 8.** Variation of the critical inner droplet fraction  $\phi^*$  for droplet–globule coalescence under different initial conditions; (a) constant oil content and variable inner droplet fractions; (b) constant globule and inner droplet fraction and variable SC concentrations. The data are upper limits deduced from the calibration curve of Fig. 7 (see text for details).

same mother emulsion diluted with oil in order to vary  $\phi_{i,0}$ . Thus, the inverted emulsions initially have the same average diameter and  $\phi_{i,0}$  determines the average number of inner droplets per globule. During the swelling process, to reach a given inner volume fraction, droplets necessarily undergo a larger size increment if they are initially fewer. This has profound consequences for the stability with respect to coalescence (Leal-Calderon, Schmitt, & Bibette, 2007; Pays et al., 2002). Droplet–globule coalescence is more likely to occur for larger drops because of their higher surface area of contact with the globule interface, and this could qualitatively explain the variation of  $\phi^*$  observed in Fig. 8-a. On the contrary, there is no significant change of  $\phi^*$  when the initial concentration of SC is varied at constant  $\phi_{i,0}$ , as can be deduced from Fig. 8-b. This is mainly reflecting the fact that the initial number of inner droplets is constant and that the osmotic conditions are not significantly varying within the explored SC concentration range.

The above-described approach based on coalescence assumes that this instability is provoked by compressive forces due to the inward flux increasing the droplet fraction. We cannot exclude that coalescence also takes place during step 3, as a result of the applied shear stress. Indeed, it has been reported (Muguet et al., 2001; Stroeve & Varanasi, 1984) that during globule breakup, a fraction of the internal aqueous droplets are expelled into the continuous phase. However, we believe this phenomenon was marginal in our case because  $\phi_{i,0}$  was always well below the random close packing fraction (from 70 to 80 vol.% for polydisperse emulsions) and also because the viscous stress applied to produce globule break-up was moderate. The applied stress,  $\tau = \eta_c \dot{\gamma}$ , where  $\eta_c$  is the viscosity of the continuous phase and  $\dot{\gamma}$  is the applied shear rate, is transmitted to the globules, which undergo elongation. The capillary number is a dimensionless parameter defined as the ratio of viscous stress to Laplace pressure,  $P_L = 4\sigma/d_g$ , where  $d_g$  is the globule diameter:

$$Ca = \frac{2\tau}{P_L} = \frac{d_g \eta_c \dot{\gamma}}{2\sigma} \quad (7)$$

In the explored conditions, the applied capillary number lies in a range between 0.7 and 3 which is sufficient to induce breakup but low enough to limit the extent of droplet–globule coalescence. Some experiments were conducted with the composition of emulsion n° 8 (Table 1) at variable shear rates during step 3:  $\dot{\gamma} = 1000, 5000$  and  $14,200 \text{ s}^{-1}$ . Almost the same final  $G'$  value was obtained at  $4^\circ\text{C}$  for the two lowest shear rates but we visually observed that it took longer time, about 30 min, to reach the gelled state like that described in Fig. 1-b at room temperature for  $\dot{\gamma} = 1000 \text{ s}^{-1}$ . This was due to the fact that average globule size was larger (50–60  $\mu\text{m}$ ) leading to lower exchange surface area and consequently slower water diffusion. At the opposite, the final  $G'$  value at  $4^\circ\text{C}$  was nearly 2-fold lower for the emulsion sheared at  $\dot{\gamma} = 12,500 \text{ s}^{-1}$ , reflecting significant droplet release during the fragmentation stage.

### 3.5. Probing the generality of the concept

In the previous sections, the overall oil fraction was fixed at 5 wt.%. One experiment was carried out at 10 wt.% oil corresponding to emulsion n° 15 in Table 1. In principle, the water intake capacity of the inner phase is twice as large as that of emulsion n° 4. The obtained material was visually firm and brittle and it was impossible to homogeneously spread it on the rheometer plate after the storage period of 15 h at  $4^\circ\text{C}$ . We had to adopt a specific protocol to characterize its mechanical properties: the double emulsion was loaded in the rheometer at  $4^\circ\text{C}$  immediately after step 3, at a stage such that swelling was not achieved and the material had sufficient plasticity. The rheological moduli were measured and the asymptotic values were  $G' \approx 1.8 \times 10^4 \text{ Pa}$  and  $G'' \approx 4.0 \times 10^3 \text{ Pa}$  after 15 h. For the sake of comparison, we obtained  $G' \approx 4.0 \times 10^3 \text{ Pa}$  and  $G'' \approx 1.6 \times 10^3 \text{ Pa}$  for emulsion n° 4. This experiment reveals that the amount of oil is also strongly influencing the final gel properties. It also illustrates the potentiality of the process to generate strong gels, while maintaining low fat level.

The generality of the concept was also proved by replacing SC by gum Arabic (GA), which is a surface-active hydrophilic biopolymer. Even at large concentration, GA exhibited low thickening and/or gelling properties. It was thus associated with Xanthan. The formulation corresponds to emulsions n° 16 in Table 1. It was fabricated following exactly the same process as that described in Section 2.2. After step 2, the emulsion was viscous but pourable under the effect of gravity. We measured its rheological properties and we found:  $G' = 16 \text{ Pa}$ ;  $G'' = 6 \text{ Pa}$ . However, after step 3, the material underwent a rheological transition from fluid to elastic paste. The final rheological moduli were  $1.0 \times 10^3 \text{ Pa}$  and  $G'' = 240 \text{ Pa}$  at  $4^\circ\text{C}$ .

## 4. Conclusion

The compartmented structure of W/O/W double emulsions and the fast water permeation through the oil phase makes it possible to monitor inflation or deflation of the aqueous compartments depending on the osmotic pressure difference. In this paper, we described a gelation phenomenon based on an osmotically driven water transfer process from the external phase to the inner droplets. Direct evidence of water transfer was given by microscope images showing interfacial undulations/protrusions due to the strong compressive forces exerted by the concentrated inner droplets on the globule surface in the final state. The external phase was a protein and/or hydrocolloid solution whose rheological

moduli  $G'$  and  $G''$  rise sharply with concentration, providing further evidence for water transfer. The inward flux tended to concentrate the biopolymers in the external phase thus favoring gel formation. Our strategy to design gelled materials was based on the fabrication of double emulsions with large globules, followed by the application of an intense shear during a short period of time (seconds). The surface area increment accelerated water transfer and gelation occurred within a few minutes. We provided evidence that the final state was determined by droplet–globule coalescence phenomena taking place during the swelling process as a result of their dense packing. The systems were characterized 15 h after fabrication but they maintained their gelled structure for at least one month when stored at 4 °C. The strategy requires the formulation of a primary W/O emulsion with high solute concentration to induce the large osmotic pressure mismatch. However, it is worth mentioning that the concentration of solute relative to the whole double emulsion mass was rather low.

We hope this study will provide a useful guidance for the formulation of texturized emulsions with low fat, salt or sugar content, as required in many food applications.

## Acknowledgments

The authors gratefully acknowledge the Aquitaine regional Council (Conseil Regional d'Aquitaine) for financial support.

## References

- Benichou, A., Aserin, A., & Garti, N. (2004). Double emulsions stabilized with hybrids of natural polymers for entrapment and slow release of active matters. *Advances in Colloid and Interface Science*, 108–109, 29–41.
- Bonnet, M., Cansell, M., Berkaoui, A., Ropers, M. H., Anton, M., & Leal-Calderon, F. (2009). Release rate profiles of magnesium from multiple W/O/W emulsions. *Food Hydrocolloids*, 23, 92–101.
- Bonnet, M., Cansell, M., Placin, F., Anton, M., & Leal-Calderon, F. (2010). Impact of protein concentration and location on ion release from multiple W/O/W emulsions. *Langmuir*, 26, 9250–9260.
- Bouchoux, A., Cayemite, P. E., Jardin, J., Gésan-Guizou, G., & Cabane, B. (2009). Casein micelle dispersion under osmotic stress. *Biophysical Journal*, 96, 693–706.
- Cheng, J., Chen, J. F., Zhao, M., Luo, Q., Wen, L. X., & Papadopoulos, K. D. (2007). Transport of ions through the oil phase of W1/O/W2 double emulsions. *Journal of Colloid and Interface Science*, 305, 175–182.
- Cole, M. L., & Whateley, T. L. (1997). Release rate profiles of theophylline and insulin from stable multiple W/O/W emulsions. *Journal of Controlled Release*, 49(1), 51–58.
- Colinart, P., Delepine, S., Trouve, G., & Renon, H. (1984). Water transfer in emulsified liquid membrane processes. *Journal of Membrane Science*, 20(2), 167–187.
- Cournarie, F., Savelli, M. P., Rosilio, V., Bretez, F., Vauthier, C., Grossiord, J. L., et al. (2004). Insulin-loaded W/O/W multiple emulsions: comparison of the performances of systems prepared with medium-chain-triglycerides and fish oil. *European Journal of Pharmaceutics and Biopharmaceutics*, 58(3), 477–482.
- Farrer, D., & Lips, A. (1999). On the self-assembly of sodium caseinate. *International Dairy Journal*, 9, 281–286.
- Fechner, A., Knoth, A., Scherze, I., & Muschiolik, G. (2007). Stability and release properties of double-emulsions stabilised by caseinate–dextran conjugates. *Food Hydrocolloids*, 21(5–6), 943–952.
- Florence, A. T., & Whitehill, D. (1982). The formulation and stability of multiple emulsions. *International Journal of Pharmaceutics*, 11(4), 277–308.
- Garti, N. (1997). Double emulsions—scope, limitations and new achievements. *Colloids and Surfaces A: Physicochemical and Engineering Aspects*, 123–124, 233–246.
- Garti, N., Magdassi, S., & Whitehill, D. (1985). Transfer phenomena across the oil phase in water–oil–water multiple emulsions evaluated by Coulter counter: 1. Effect of emulsifier 1 on water permeability. *Journal of Colloid and Interface Science*, 104(2), 587–591.
- Garti, N., Romano-Pariente, A., & Aserin, A. (1987). The effect of additives on release from W/O/W emulsions. *Colloids and Surfaces*, 24, 83–94.
- Hino, T., Yamamoto, A., Shimabayashi, S., Tanaka, M., & Tsujii, D. (2000). Drug release from W/O/W emulsions prepared with different chitosan salts and concomitant creaming up. *Journal of Controlled Release*, 69(3), 413–419.
- Jager-Lezer, N., Terrisse, I., Bruneau, F., Tokgoz, S., Ferreira, L., Clausse, D., et al. (1997). Influence of lipophilic surfactant on the release kinetics of water-soluble molecules entrapped in a W/O/W multiple emulsion. *Journal of Controlled Release*, 45, 1–13.
- Kita, Y., Matsumoto, S., & Yonezawa, D. (1978). Permeation of water through the oil layer in W/O/W-type multiple-phase emulsions. *Nippon Kagaku Kaishi*, 1, 11.
- Laugel, C., Baillet, A., Youenang Piemi, M. P., Marty, J. P., & Ferrier, D. (1998). Oil–water–oil multiple emulsions for prolonged delivery of hydrocortisone after topical application: comparison with simple emulsions. *International Journal of Pharmaceutics*, 160(1), 109–117.
- Laugel, C., Chaminade, P., Baillet, A., Seiller, M., & Ferrier, D. (1996). Moisturising substances entrapped in W/O/W emulsions: analytical methodology for formulation, stability and release studies. *Journal of Controlled Release*, 38(1), 59–67.
- Leal-Calderon, F., Homer, S., Goh, A., & Lundin, L. (2012). W/O/W emulsions with high internal droplet volume fraction. *Food Hydrocolloids*, 27, 30–41.
- Leal-Calderon, F., Schmitt, V., & Bibette, J. (2007). *Emulsion science. Basic principles. 2nd version*. Springer-Verlag.
- Lobato-Calleros, C., Rodriguez, E., Sandoval-Castilla, O., Vernon-Carter, E. J., & Alvarez-Ramirez, J. (2006). Reduced-fat white fresh cheese-like products obtained from W1/O/W2 multiple emulsions: viscoelastic and high-resolution image analyses. *Food Research International*, 39(6), 678–685.
- Mabille, C., Schmitt, V., Gorria, P., Leal-Calderon, F., Faye, V., Deminière, et al. (2000). Rheological and shearing conditions for the preparation of monodisperse emulsions. *Langmuir*, 16(2), 422–429.
- Mabille, C., Leal-Calderon, F., Bibette, J., & Schmitt, V. (2003). Monodisperse fragmentation in emulsions: mechanism and kinetics. *Europhysics Letters*, 61, 708–714.
- Marze, S. (2009). Relaxation processes of PGPR at the Water/Oil interface inferred by oscillatory or transient viscoelasticity measurements. *Langmuir*, 25(20), 12066–12072.
- Matsumoto, S., Inoue, T., Kohda, M., & Ikura, K. (1980). Water permeability of oil layers in W/O/W emulsions under osmotic pressure gradients. *Journal of Colloid and Interface Science*, 77(2), 555–563.
- Matsumoto, S., & Kohda, M. (1980). The viscosity of W/O/W emulsions: an attempt to estimate the water permeation coefficient of the oil layer from the viscosity changes in diluted systems on aging under osmotic pressure gradients. *Journal of Colloid and Interface Science*, 73(1), 13–20.
- Mezzenga, R. (2007). Equilibrium and non-equilibrium structures in complex food systems. *Food Hydrocolloids*, 21(5–6), 674–682.
- Mezzenga, R., Folmer, B. M., & Hughes, E. (2004). Design of double emulsions by osmotic pressure tailoring. *Langmuir*, 20(9), 3574–3582.
- Muguet, V., Seiller, M., Barratt, G., Ozer, O., Marty, J. P., & Grossiord, J. L. (2001). Formulation of shear rate sensitive multiple emulsions. *Journal of Controlled Release*, 70(1–2), 37–49.
- Pays, K., Giermanska-Kahn, J., Pouligny, B., Bibette, J., & Leal-Calderon, F. (2002). Double emulsions: how does release occur? *Journal of Controlled Release*, 79(1–3), 193–205.
- Raynal, S., Pezron, I., Potier, L., Clausse, D., Grossiord, J. L., & Seiller, M. (1994). Study by differential scanning calorimetry, rheometry and electroconductimetry of mass transfers at subambient and ambient-temperatures in multiple water/oil/water emulsions entrapping MgSO<sub>4</sub>. *Colloids and Surfaces A: Physicochemical and Engineering Aspects*, 91, 191–205.
- Shima, M., Morita, Y., Yamashita, M., & Adachi, S. (2006). Protection of *Lactobacillus acidophilus* from the low pH of a model gastric juice by incorporation in a W/O/W emulsion. *Food Hydrocolloids*, 20(8), 1164–1169.
- Stroevé, P., & Varanasi, P. P. (1984). An experimental study on double emulsion drop breakup in uniform shear flow. *Journal of Colloid and Interface Science*, 99, 360–373.
- Tedajo, G. M., Bouttier, S., Fourniat, J., Grossiord, J.-L., Marty, J. P., & Seiller, M. (2005). Release of antiseptics from the aqueous compartments of a W/O/W multiple emulsion. *International Journal of Pharmaceutics*, 288(1), 63–72.
- Wen, L., & Papadopoulos, K. D. (2000). Effects of surfactants on water transport in W1/O/W2 emulsions. *Langmuir*, 16(20), 7612–7617.